



Oxygen fugacity, temperature and pressure estimation from mineral chemistry of the granodiorite porphyry from the Jilongshan Au-Cu deposit and the Baiguoshu prospecting area in SE Hubei Province: A guide for mineral exploration

Bakaramoko Samake^a, Yao-Ming Xu^{a,*}, Shao-Yong Jiang^{a,b,***}

^a State Key Laboratory of Geological Processes and Mineral Resources, Faculty of Earth Resources, Collaborative Innovation Center for Exploration of Strategic Mineral Resources, China University of Geosciences, Wuhan 430074, China

^b State Key Laboratory of Mineral Deposits Research, Department of Earth Sciences, Nanjing University, Nanjing 210093, China



ARTICLE INFO

Keywords:

Minerals chemistry
Oxygen fugacity
Pressure
Temperature
Baiguoshu prospect
Jilongshan Cu-Au deposit

ABSTRACT

The Jilongshan Au-Cu deposit is located in the Jiurui district of the Middle-Lower Yangtze River Metallogenic Belt in the south-eastern part of Hubei Province and close to the northern border of Jiangxi Province. This study focuses on mineral chemistry of biotite, amphibole and plagioclase in the ore-related granodiorite porphyry at the Jilongshan deposit and similar porphyry rock from the nearby Baiguoshu prospect, in an attempt to investigate the mineralization potential in the Baiguoshu area. The biotites from the Jilongshan and Baiguoshu granodiorite porphyries all belong to magnesian-biotite but the Jilongshan contains higher Mg. The calculation of Fe^{3+} and Fe^{2+} of the biotites indicated that the Jilongshan pluton shows higher oxygen fugacity that is favorable for Cu-Au mineralization, whereas the Baiguoshu pluton shows lower $f\text{O}_2$. The Jilongshan amphiboles show higher Mg / (Mg + Fe) and lower Si which mainly belong to magnesiohornblende, whereas the Baiguoshu accommodates mainly the tschermakite. The plagioclases of the Jilongshan and Baiguoshu plutons show no compositional difference and both belong to andesine. The calculated temperatures and pressures by the co-existing amphibole-plagioclase pairs indicate that average crystallization temperature of the Jilongshan pluton is 624–736 °C and the pressure is low at 0.5–0.9 kbar, in contrast the Baiguoshu pluton shows higher temperature of 724–832 °C and higher pressure of 3.2–6.3 kbar. These data suggest that the Baiguoshu pluton has less mineralization potential than the Jilongshan pluton, therefore the Baiguoshu prospect shows less economic importance and further exploration should be carried out at depth in the Jilongshan area.

1. Introduction

The Middle-Lower Yangtze River Metallogenic Belt (MLYRMB), which is located at the crossing points of the northern side of the Yangtze Craton, the Dabieshan orogenic belt, and the southern border of the North China Craton, is considered as one of the economically most important metallogenic belt in China (Pan and Dong, 1999). This belt accommodates > 200 Mesozoic magmatic-hydrothermal poly-metallic deposits, and is composed of seven ore-concentrated districts from west to east including Edong (SE Hubei Province) Fe–Cu deposits, Jiurui (Jiujiang–Ruichang) Cu–Au–Mo deposits, Anqing–Guichi Cu deposits, Luzong (Lujiang–Zongyang) Fe–Cu deposits, Tongling Cu–Au deposits, Ningwu (Nanjing–Wuhu) Fe deposits and Ningzhen (Nanjing–

Zhenjiang) Cu–Fe–Pb–Zn deposits (Fig. 1) (Zhai et al., 1996; Zhao et al., 1999). Most of these deposits and related intrusive rocks were formed within a 10 Ma period around 140 Ma (Sun et al., 2003; Ding et al., 2005; Mao et al., 2006; Jiang et al., 2008; Li and Jiang, 2009; Xie et al., 2009; Li et al., 2010; Yang et al., 2011; Jiang et al., 2013; Zhu et al., 2014). The belt has been extensively investigated during the past decades and previous work outlines that the Yanshanian (late Mesozoic) magmatism in general dominated the mineralization (Chang et al., 1991; Zhai et al., 1996; Jiang et al., 2008, 2013). Three kinds of magmatic rocks are related to different types of deposits in this belt, including: (1) high-K calc-alkaline, intermediate to felsic intrusive rocks (consisting mainly of diorite, quartz diorite, granodiorite and corresponding porphyries) related to skarn and porphyry Cu–Au–Mo

* Corresponding author.

** Correspondence to: S.Y. Jiang, State Key Laboratory of Geological Processes and Mineral Resources, Faculty of Earth Resources, Collaborative Innovation Center for Exploration of Strategic Mineral Resources, China University of Geosciences, Wuhan 430074, China.

E-mail addresses: ymxu@cug.edu.cn (Y.-M. Xu), shyjiang@cug.edu.cn (S.-Y. Jiang).

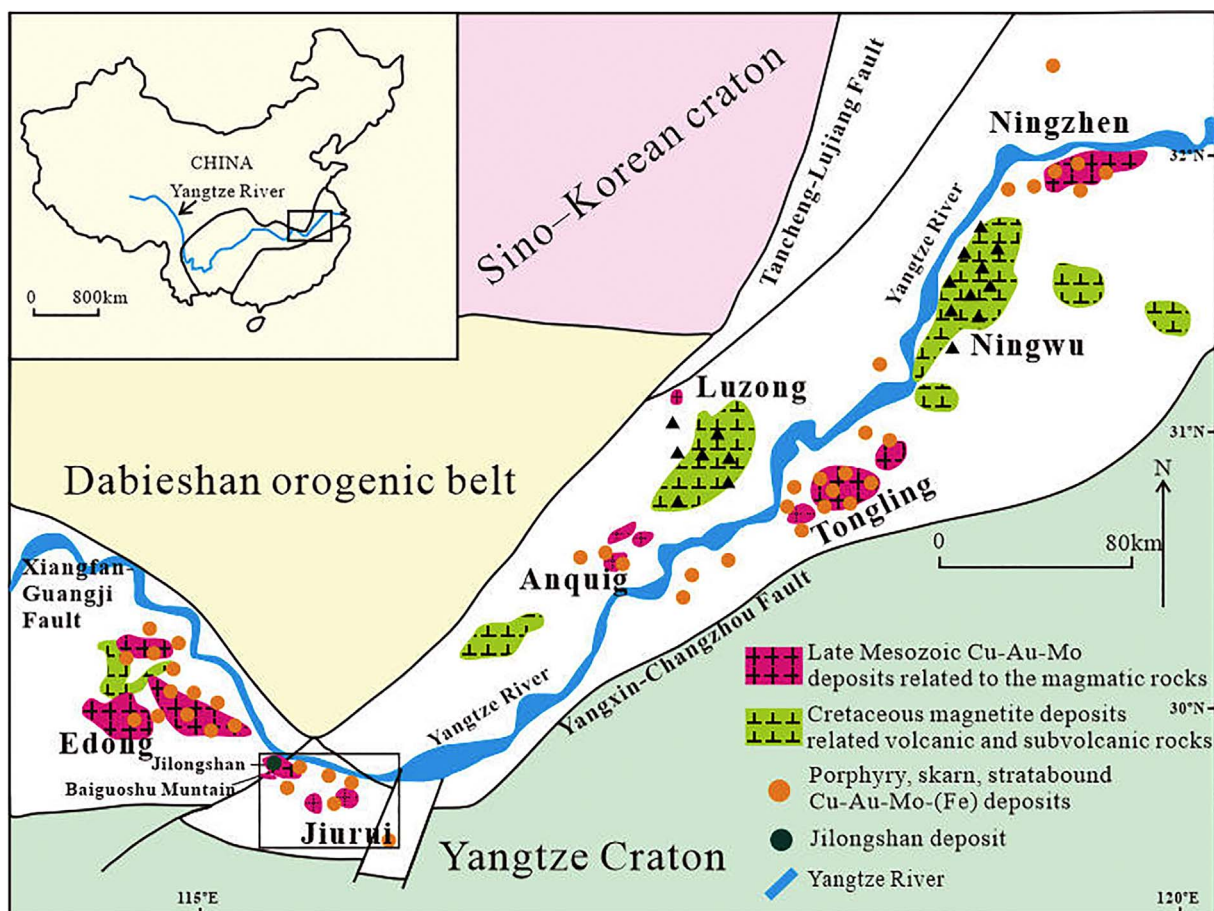


Fig. 1. Geological sketch map of the Middle–Lower Yangtze River Metallogenic Belt.

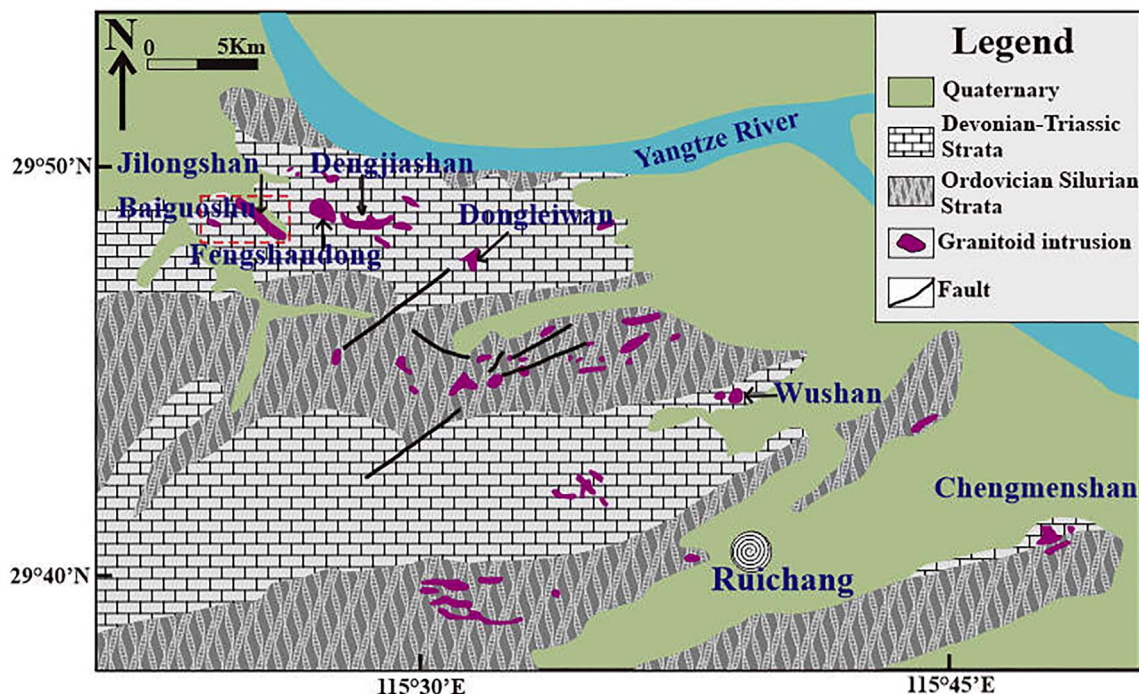


Fig. 2. Geological sketch map of the Juirui ore district.

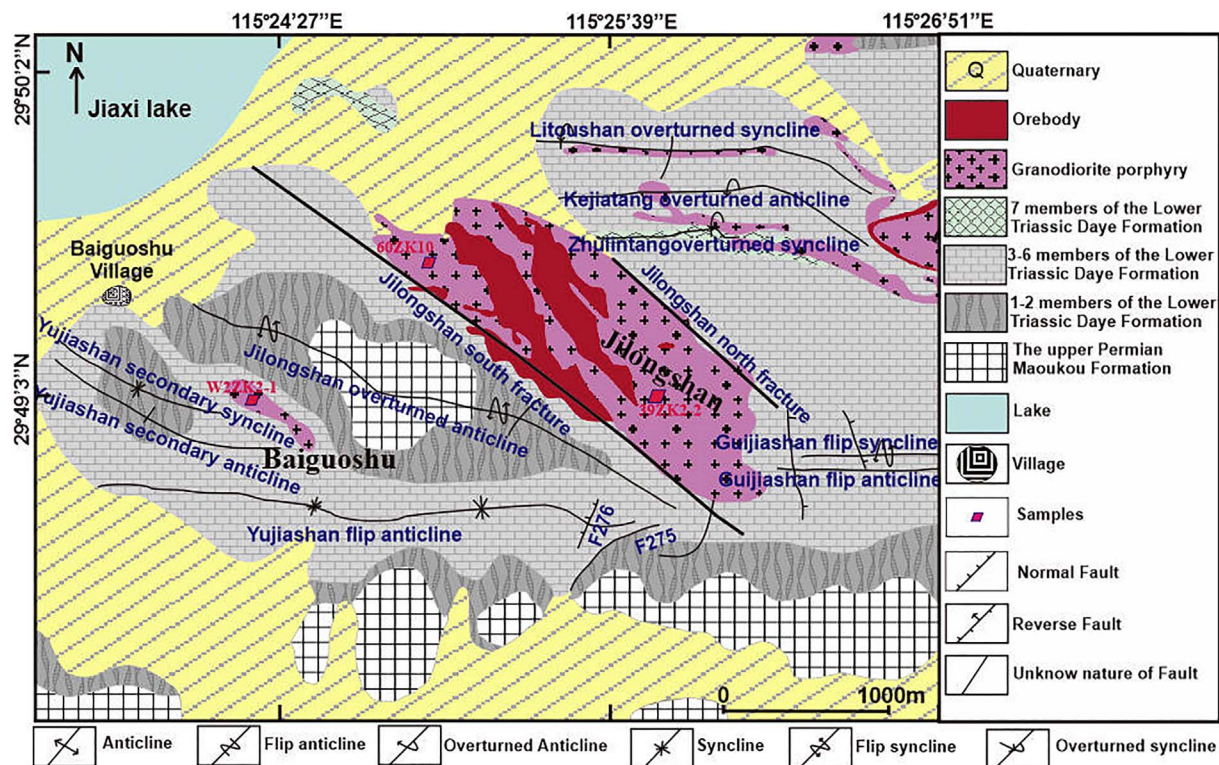


Fig. 3. Geological sketch map of the Jilongshan and Baiguoshu regions, Hubei Province.
(modified after Mo et al., 2011; Pang et al., 2014).

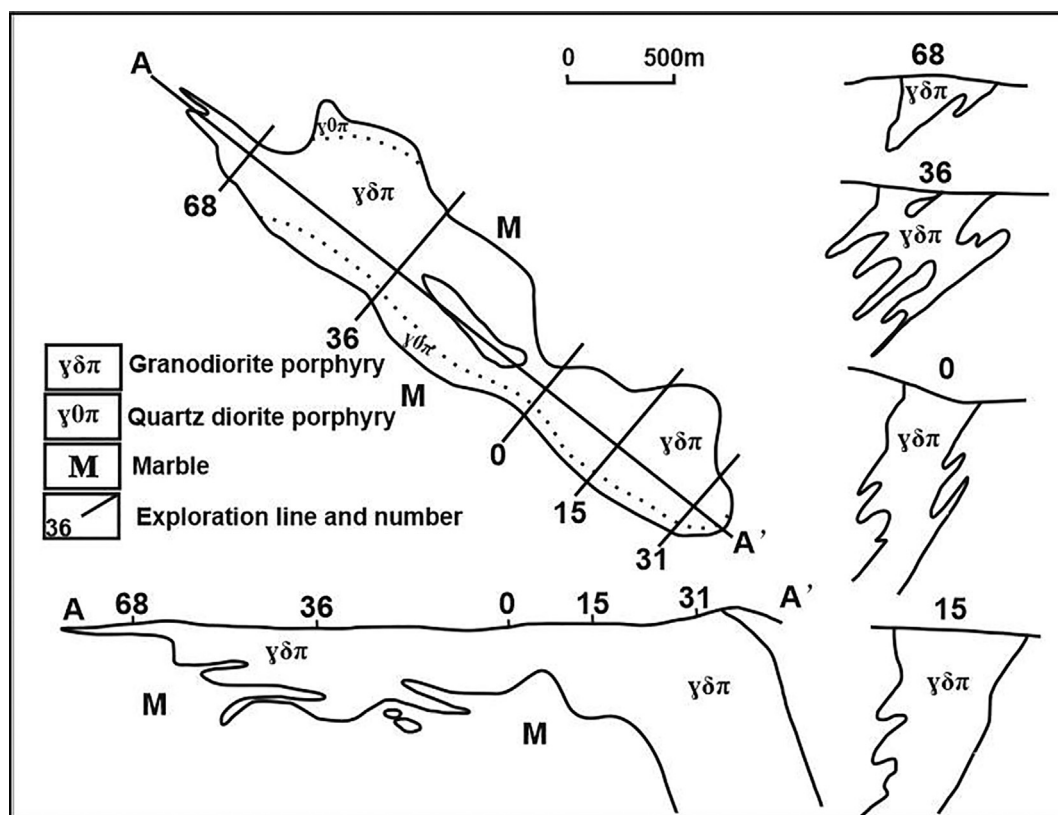


Fig. 4. A sketch map for the plane and cross section morphology of the Jilongshan pluton.

Table 1

Comparison of the Jilongshan and Baiguoshu granodiorite porphyry and ore deposit geology.

	Jilongshan	Baiguoshu	References
Intrusive	Granodiorite	Granodiorite	Pang et al. (2014),
Colour	Grey	Grey-green	This study
Grain size	Inequigranular	Inequigranular	
Structure	Massive	Massive	
Texture	Porphyritic	Porphyritic	
Phenocryst	Bio, pl, amp, Kfeldspar, Qz...	Bio, pl, amp...	
Ground mass	Inequigranular with size around 0.05 to 0.3 mm	Inequigranular with grain size about 0.01 to 0.03 mm	
Deposit type	Skarn type, Porphyry type, Minor marble type	None	Bi and Yang (2008), Wang et al. (2014), Pang et al. (2014), This study
Metal minerals	Chalcopyrite, pyrite, galena, sphalerite, molybdenite, magnetite, hematite, pyrrhotite, rhodochrosite, bornite, orpiment, realgar.	None	Bi and Yang (2008), Wang et al. (2014), Pang et al. (2014)
Other minerals	Garnet, diopside, calcite, quartz, chlorite, sericite, phlogopite, fluorite, tremolite, actinolite, serpentine, talc, pyrophyllite, kaolinite, epidote	None	Bi and Yang (2008); Wang et al. (2014), Pang et al. (2014)
Ore types	Cu-Mo(Au), Cu-Au-Ag, Au-Pb-Zn, Ag-Au (As), Te-Au	None	Bi and Yang (2008), Wang et al. (2014), Pang et al. (2014)
Ore tonnage and grade	Ore: 19.75Mt Au: 42 t with 4 g/t Au Cu: 270,000 t with 1.6% Cu Ag: 380 t with 19 g/t Ag	None	Internal Report from Team of Zhongan Metallurgical Survey, Khin et al. (2007)

deposits; (2) Na-rich calc-alkaline, intermediate to felsic intrusive rocks (mainly comprising pyroxene diorite porphyry, diorite porphyry) related to skarn and magmatic-hydrothermal Fe–Cu–Au deposits; (3) andesitic rocks in the volcanic basin, connected with porphyry Fe deposits outlined by the investigations in Wuhu and Ningwu areas (Chang et al., 1991; Zhai et al., 1996; Pan and Dong, 1999).

In the Jiurui district, the late Mesozoic (Yanshanian) magmatic rocks belong to a medium to high-K metaluminous calc-alkaline rock (Zhai et al., 1996; Jiang et al., 2013). The main rock types include granodiorite porphyry and quartz diorite porphyry, with minor amounts of diorite, quartz porphyry, monzogranite and granite porphyry. The most important ore deposits in the Jiurui district from east to west include: Chemgmenshan, Wusha, Dongleiwan, Dengjiashan, Fengshandong and Jilongshan deposits (Fig. 2). In the Baiguoshu area there are occurrences of similar granodiorite porphyry as in nearby Jilongshan Au–Cu deposit that are separated by a major NW-trending fault (Fig. 3), and mineral exploration activity is currently on-going in this region. Jilongshan deposit accommodates approximatively 20 Mt ore with a large scale of gold deposit with ~50 t Au and a medium size copper deposit with > 290,000 t of Cu and 380 t of Ag at a grade of 19 g/t Ag. However, the Baiguoshu pluton is still an ore barren pluton at present (Khin et al., 2007). The principal objective of this study is to compare the chemical characteristics of the ore-related Jilongshan pluton and the nearby Baiguoshu pluton to explore the mineralization potential in the Baiguoshu area, using chemical compositions of biotite, amphibole and plagioclase in the intrusive rocks. The results will contribute to our understanding of crystallization conditions such as oxygen fugacity, pressure and temperature which are also key factors that may control the porphyry-type Cu–Au mineralization (Richards, 2015).

2. Geological background

The MLYRMB is located in the northern part of Yangtze Craton and is bordered by three important faults: northwest by Xiangfan-Guangji Fault (XGF) limiting this famous belt to the Dabieshan orogenic belt, northeast by the Tancheng-Lujiang regional strike-slip Fault (TLF) dividing the belt and the North China Craton and the Dabieshan belt and also the Yangxin-Changzhou Fault (YCF) separate it to Yangtze Craton

in the south (Fig. 1). The basement is generally characterized by the Paleoproterozoic to Archean formations including biotite–amphibole gneisses, tonalites, trondjemites, granodiorites and supracrustal rocks all metamorphosed to amphibolite and granulite facies with pervasive migmatization but they are poorly exposed (Pan and Dong, 1999). The basement is covered by Paleoproterozoic to Neoproterozoic volcanosedimentary rocks including calc-alkaline basalts, rhyolitic rocks and marine carbonate and clastic sedimentary rocks that can be metamorphosed to schists and gneisses (Chang et al., 1991). The ages of the Yanshanian igneous rocks in the MLYRMB range from 150 to 120 Ma (Mao et al., 2006; Hu and Jiang, 2010; Li et al., 2010; Yang et al., 2011; Jiang et al., 2013; Pang et al., 2014; Wang et al., 2014).

The Jiurui district is situated at the southernmost transitional points of the arcuate structure of the MLYRMB (Fig. 1). This ore district accommodates more than ten deposits with four large ones (Jilongshan Au–Cu, Fengshandong Cu–Mo, Wushan Cu–Au and Chengmenshan Cu–Au–Mo). The late Proterozoic metamorphic rocks represent the crystalline basement of the region which are not well crop out. The well exposed sedimentary strata in the Jiurui district are Ordovician, Silurian, Devonian, Carboniferous, Permian, Triassic and Quaternary (Fig. 2), and are composed of limestone, dolomitic limestone, dolomite, sandstone and shale.

The Jilongshan Au–Cu deposit is located in the westernmost part of the Jiurui district with one of the six largest exposed plutons (Jilongshan, Fengshandong, Dengjiashan, Dongleiwan, Wushan and Chengmenshan) at Jiurui (Fig. 2). The intrusive rocks are characterized by the granodiorite porphyry, quartz diorite, and some intermediate-felsic rocks and have a surface exposed area of 1.8 km² (Mo et al., 2011). The main exposed sedimentary strata in the area include the Lower Triassic Daye Formation (Members 1 to 7) of limestone, dolomitic limestone and dolomite, the Upper Permian Maokou Formation of limestone and the Quaternary of sand, gravel, clay and soil (Zhao et al., 1999; Mo et al., 2011). The Jilongshan-Baiguoshu area is structurally complex and characterized by well-developed folds and faults (Fig. 3). These folds are linear overturned, flip anticline and syncline, for example, the Kejidian and Zhulintang are overturned anticline, the Guijiashan is characterized by flip anticline and syncline, and the Jilongshan is characterized by flip anticline (Pang et al., 2014). The brittle deformations are NW

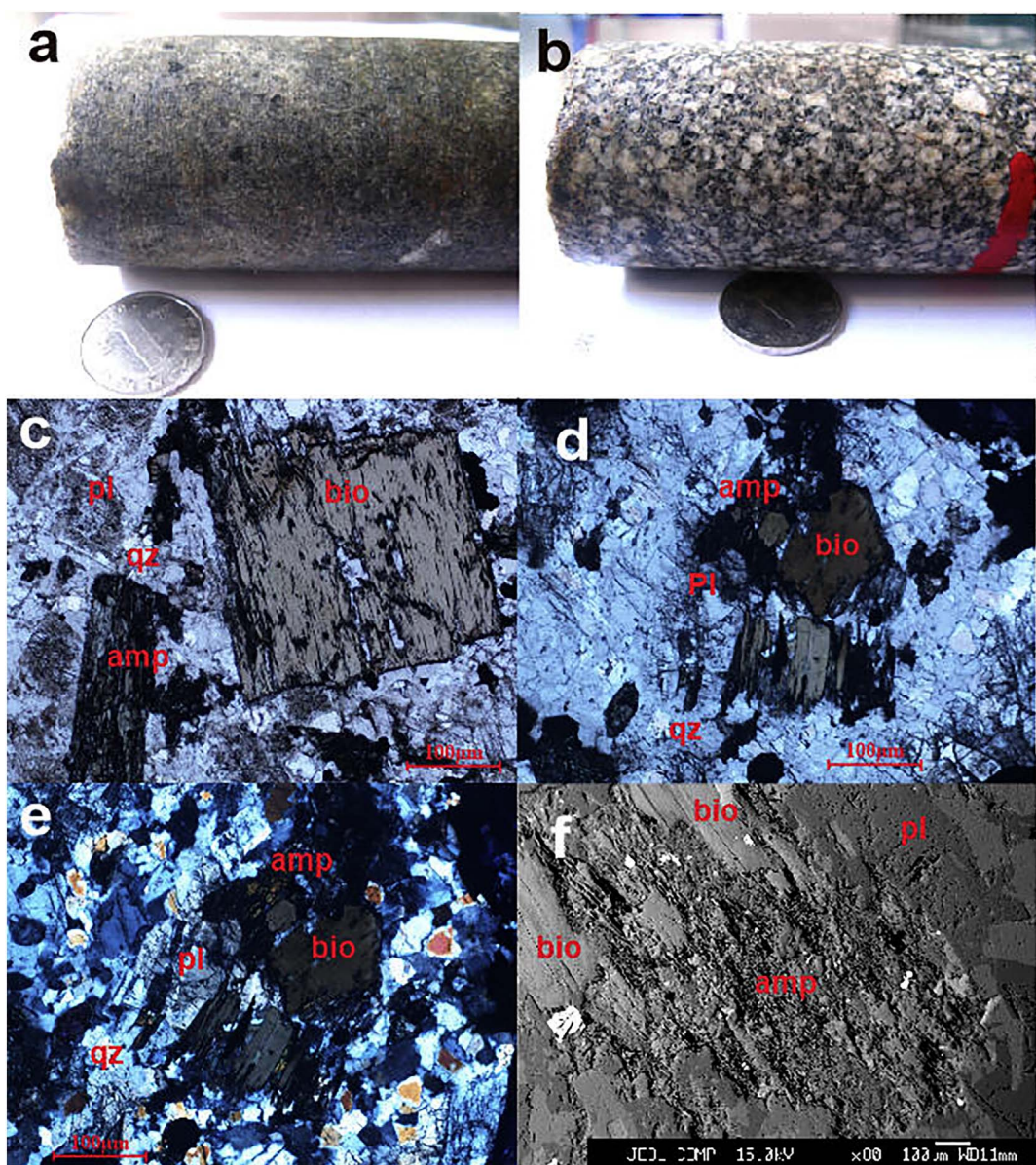


Fig. 5. Photos of the Jilongshan pluton samples. a) Granodiorite porphyry from Jilongshan drilling core 60ZK10; b) Quartz diorite porphyry; c,d,e) Photomicrographs of polished thin sections of the Jilongshan granodiorite porphyry presenting amphibole, plagioclase, quartz and biotite; f) SEM photo of the Jilongshan thin section with disaggregated amphibole.

compressional, NNW and EW tensional (Pan and Dong, 1999; Mo et al., 2011; Pang et al., 2014). The Jilongshan pluton is a composite intrusion and is shaped in horizontal section as a barbell and looks like mushroom in vertical sections (Fig. 4). These rocks show a peraluminous, high-K calc-alkaline characteristic typical of granitoids associated with skarn and porphyry Cu–Au–Mo polymetallic deposits and the emplacement age is 151.7 ± 0.7 Ma (Pang et al., 2014).

In the Jilongshan deposit, the main ore bodies occur both at the contact area between the Triassic Daye limestone and the granodiorite porphyry and within the porphyry body (Fig. 3). The mineralization types include mainly skarn-type, granodiorite porphyry-type, and minor marble-type (Zhao et al., 1999). The ore minerals include chalcopyrite, pyrite, magnetite, malachite, azurite, bornite and molybdenite. Re–Os dating of molybdenite from the Jilongshan deposit shows an age of 150.8 ± 0.8 Ma, which is identical to the age of the ore-bearing granodiorite porphyry (Pang et al., 2014).

The Baiguoshu granodiorite porphyry occurs southwestern of the Jilongshan Au–Cu deposit, which also intruded into the Triassic Daye

limestone (Fig. 3). The shape of the Baiguoshu pluton is similar to the Jilongshan pluton but with smaller outcrops (Fig. 3). A comparison of the Jilongshan and Baiguoshu granodiorite porphyry and ore deposit geology is listed in Table 1.

3. Petrography

The samples we collected from the Jilongshan pluton include granodiorite porphyry and quartz diorite porphyry. The granodiorite porphyry samples at Jilongshan are grey, porphyritic texture, inequigranular with massive structure (Fig. 5a). The quartz diorite porphyry shows grey-green colour, porphyritic texture and massive structure, and the phenocrysts include mainly plagioclase, and some amphibole and biotite (Fig. 5b). In the granodiorite porphyry, the phenocrysts constitute mainly plagioclase, K-feldspar, amphibole, and biotite (Fig. 5c, d). Most of the plagioclases are prismatic, platy and present polysynthetic twin structure, interpenetration twin and girdle texture. The amphiboles are prismatic and rhombic, dark green colour

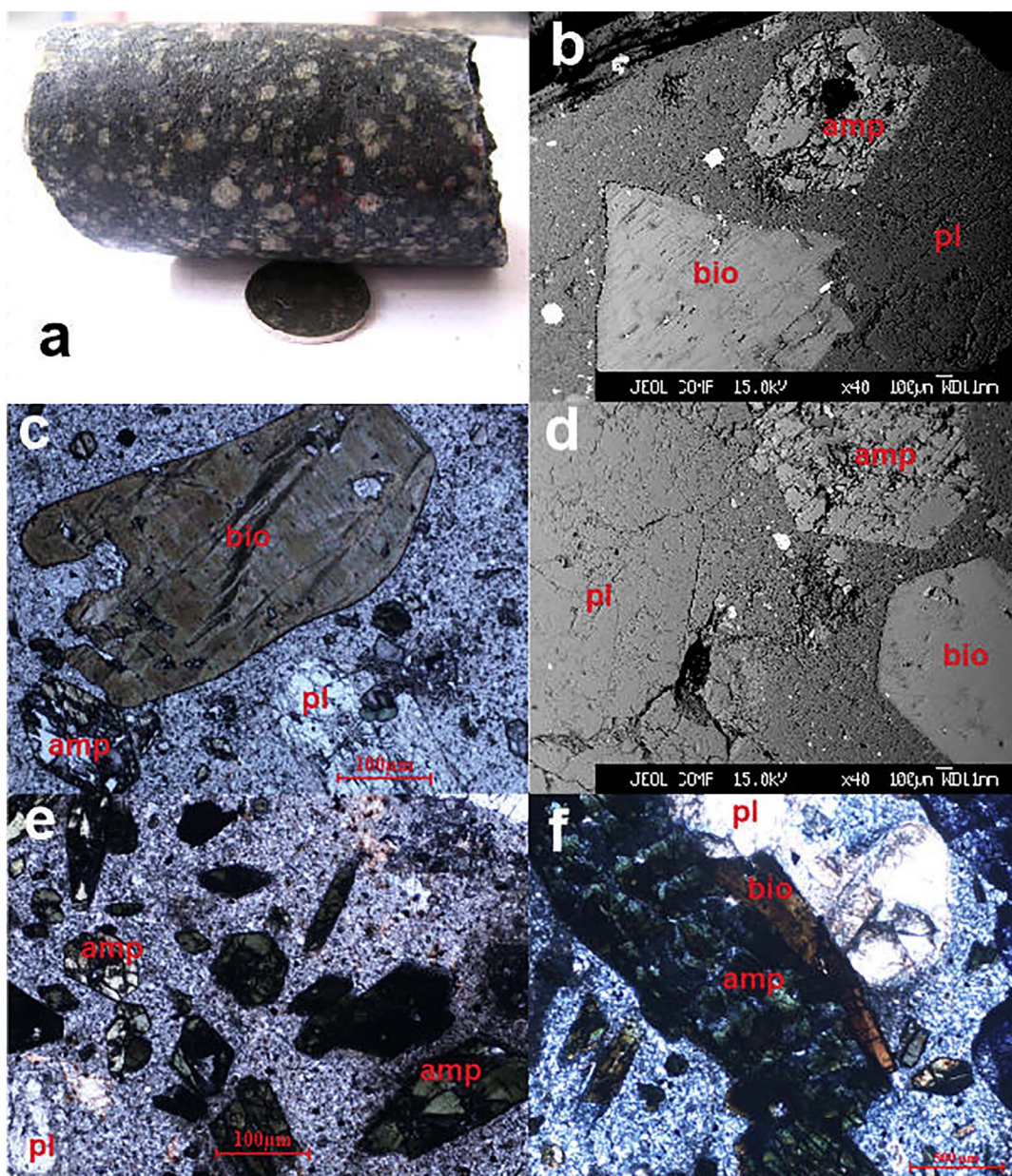


Fig. 6. Photos of the Baiguoshu pluton samples. a) Granodiorite porphyry from the Baiguoshu drilling core W2ZK2; b) SEM photo of the Baiguoshu thin section showing sub-euhedral amphibole; c) Photomicrograph of polished thin sections of the Baiguoshu pluton, showing rock textures and accommodated minerals of biotite, amphibole and plagioclase; d) SEM photo of the Baiguoshu thin section showing euhedral amphibole and biotite; e) abundant and small-sized amphiboles; f) coexisting amphibole, biotite and plagioclase.

and coexist with plagioclases (Fig. 5c–f). The biotites are anheudral, schistose or hexagonal; they are partially altered (Fig. 5d, e). Quartz grains are granular and anheudral (Fig. 5c–e). The groundmass with anheudral grain-size of about 0.05–0.3 mm contains the same mineral assemblages as the phenocrysts (Fig. 5c–f).

The samples from Baiguoshu pluton are characterized by grey-green colour, inequigranular with porphyritic texture and massive structure (Fig. 6a). The phenocrysts comprise mainly of euhedral and sub-euhedral plagioclases (Fig. 6a). The amphiboles show mostly euhedral (Fig. 6b–d), light green colour (Fig. 6e–f). The biotites are euhedral (Fig. 6b–d). The fine groundmass shows a grain-size about 0.01 mm and presents micro-granitic texture with the same mineral assemblages as the phenocrysts (Fig. 6c–f).

4. Samples and analytical method

Biotite, amphibole and feldspar samples from ten thin-sections have been analysed for their chemical compositions by the Electron Microprobe Analyser (EMPA) at the State Key Laboratory of China University of Geosciences in Wuhan (Tables 2–5). Samples for this study have been collected from drill cores and underground tunnels in the Jilongshan mining area and also in the Baiguoshu pluton.

The JEOL JXA-8100 EMPA was equipped with four wavelength-dispersive spectrometers (WDS). The accelerating voltage was about 15 kV with a beam current of 20 nA and a 1–5 µm focused electron beam was used to analyse the target minerals. The data were corrected online using a modified ZAF (atomic number, absorption, fluorescence) correction procedure. Element peaks and backgrounds were measured

Table 2

Electron microprobe analyses and structural formula of biotite from the Jilongshan and Baiguoshu granodiorite porphyry (wt%).

Samples	Jilongshan												
	z52b1	z53b1	z53b2	z55b1	z103b1	z102b1	z102b2	z42b1	z43b1	z46b1	z22b1	z23b1	z24b1
SiO ₂	36.98	36.39	36.68	36.89	39.13	37.72	37.1	37.39	37.83	37.84	37.18	37.67	37.53
TiO ₂	4.39	4.52	4.68	4.46	4.42	3.94	3.88	4.48	4.58	4.62	4.53	4.62	4.77
Al ₂ O ₃	14.51	14.17	14.32	14.38	15.46	14.81	14.58	14.32	14.2	14.64	13.94	14.09	14.16
FeO	16.58	16.15	16.21	16.17	10.35	16.05	16.73	15.98	16.66	17.07	16.8	16.66	16.48
MnO	0.3	0.32	0.33	0.29	0.34	0.32	0.31	0.27	0.32	0.32	0.21	0.22	0.24
MgO	14.65	13.69	14.13	14.9	17.26	13.4	13.17	14.03	13.64	13.78	13.54	14.05	13.89
CaO	0.11	0.14	0.18	0.2	0.14	0	0	0.03	0.02	0.06	0	0.07	0.04
Na ₂ O	0.22	0.24	0.27	0.24	0.13	0.29	0.33	0.3	0.29	0.29	0.27	0.27	0.3
K ₂ O	8.28	8.77	8.62	8.39	9.64	9.33	9.56	9.52	9.3	9.02	9.42	9.51	9.35
Total	96.01	94.39	95.42	95.91	96.87	95.86	95.66	96.31	96.83	97.62	95.88	97.16	96.76
Si	2.68	2.71	2.69	2.68	2.78	2.79	2.76	2.74	2.76	2.73	2.74	2.74	2.73
Ti	0.24	0.25	0.26	0.24	0.24	0.22	0.22	0.25	0.25	0.25	0.25	0.25	0.26
Al	1.24	1.24	1.24	1.23	1.29	1.29	1.28	1.24	1.22	1.24	1.21	1.21	1.22
Fe	1	1.01	0.99	0.98	0.61	0.99	1.04	0.98	1.02	1.03	1.04	1.01	1
Mn	0.02	0.02	0.02	0.02	0.02	0.02	0.02	0.02	0.02	0.02	0.01	0.01	0.01
Mg	1.58	1.52	1.54	1.61	1.83	1.47	1.46	1.53	1.48	1.48	1.49	1.52	1.51
Ca	0.01	0.01	0.01	0.02	0.01	0	0	0	0	0	0.01	0	0
Na	0.03	0.03	0.04	0.03	0.02	0.04	0.05	0.04	0.04	0.04	0.04	0.04	0.04
K	0.76	0.83	0.81	0.78	0.87	0.88	0.91	0.89	0.86	0.83	0.89	0.88	0.87
Al ^{IV}	1.24	1.24	1.24	1.23	1.22	1.21	1.24	1.24	1.22	1.24	1.21	1.21	1.22
Al ^{VI}	0	0	0	0	0.07	0.08	0.04	0	0	0	0	0	0
Mg/Fe + Mg	0.61	0.6	0.61	0.62	0.75	0.6	0.58	0.61	0.59	0.59	0.59	0.6	0.6
Fe ³⁺ /Fe ³⁺ + Fe ²⁺	0.59	0.45	0.52	0.59	0.4	0.22	0.23	0.35	0.35	0.41	0.36	0.38	0.4
Fe ³⁺	0.59	0.45	0.51	0.58	0.24	0.22	0.24	0.35	0.35	0.42	0.37	0.39	0.4
Fe ²⁺	0.41	0.55	0.48	0.4	0.37	0.77	0.8	0.63	0.66	0.6	0.66	0.63	0.61
Mg	1.58	1.52	1.54	1.61	1.83	1.47	1.46	1.53	1.48	1.48	1.49	1.52	1.51
Fe ³⁺ %	0.23	0.18	0.2	0.22	0.1	0.09	0.1	0.14	0.14	0.17	0.15	0.15	0.16
Fe ²⁺ %	0.16	0.22	0.19	0.16	0.15	0.31	0.32	0.25	0.26	0.24	0.26	0.25	0.24
Mg%	0.61	0.6	0.61	0.62	0.75	0.6	0.58	0.61	0.59	0.59	0.6	0.6	0.6
2Fe ²⁺ + 3Fe ³⁺	2.6	2.46	2.5	2.54	1.47	2.2	2.32	2.3	2.39	2.48	2.45	2.41	2.41
Fe ²⁺ + Fe ³⁺	1.00	1.01	0.99	0.98	0.61	0.99	1.04	0.98	1.02	1.03	1.04	1.01	1.00
Mg =	1.58	1.52	1.54	1.61	1.83	1.47	1.46	1.53	1.48	1.48	1.49	1.52	1.51
Al ^{VI} + Fe ³⁺ + Ti	0.83	0.71	0.77	0.82	0.55	0.51	0.5	0.59	0.61	0.68	0.63	0.64	0.66
Fe ²⁺ + Mn	0.18	0.24	0.21	0.17	0.17	0.33	0.34	0.27	0.28	0.26	0.28	0.26	0.26
Sum	2.59	2.46	2.52	2.61	2.55	2.32	2.3	2.39	2.37	2.42	2.39	2.42	2.42
Mg%	0.61	0.62	0.61	0.62	0.72	0.64	0.64	0.64	0.62	0.61	0.62	0.63	0.62
(Al ^{VI} + Fe ³⁺ + Ti)%	0.32	0.29	0.31	0.32	0.22	0.22	0.22	0.25	0.26	0.28	0.26	0.26	0.27
(Fe ²⁺ + Mn)%	0.07	0.1	0.08	0.07	0.07	0.14	0.15	0.11	0.12	0.11	0.12	0.11	0.11

Samples	Baiguoshu							
	w35b1	w33b1	w31b1	w21b1	w22b1	w24b1	w12b1	w13b1
SiO ₂	35.7	35.08	35.94	35.99	36.95	36.1	36.51	36.37
TiO ₂	3.91	3.84	3.76	3.81	3.76	3.85	3.73	3.75
Al ₂ O ₃	14.75	14.62	14.58	14.52	14.57	14.38	14.81	14.9
FeO	20.51	20.62	20.82	20.77	19.33	20.41	20.91	20.32
MnO	0.29	0.29	0.26	0.25	0.24	0.31	0.23	0.32
MgO	10.66	10.79	10.73	10.36	11.54	11.08	11.11	11.65
CaO	0.09	0.1	0	0.08	0	0.04	0.04	0.1
Na ₂ O	0.38	0.32	0.4	0.33	0.38	0.38	0.32	0.4
K ₂ O	9.12	8.89	9.21	9.14	9.2	9.15	9.12	8.94
Total	95.42	94.55	95.7	95.25	95.96	95.7	96.78	96.74
Si	2.71	2.68	2.72	2.74	2.77	2.73	2.72	2.7
Ti	0.22	0.22	0.21	0.22	0.21	0.22	0.21	0.21
Al	1.32	1.32	1.3	1.3	1.29	1.28	1.3	1.3
Fe	1.3	1.32	1.32	1.32	1.21	1.29	1.3	1.26
Mn	0.02	0.02	0.02	0.02	0.02	0.02	0.01	0.02
Mg	1.21	1.23	1.21	1.18	1.29	1.25	1.24	1.29
Ca	0.01	0.01	0	0.01	0	0	0	0.01
Na	0.06	0.05	0.06	0.05	0.05	0.06	0.05	0.06
K	0.88	0.87	0.89	0.89	0.88	0.88	0.87	0.85
Al ^{IV}	1.29	1.32	1.28	1.26	1.23	1.27	1.28	1.3
Al ^{VI}	0.03	0	0.02	0.05	0.06	0.01	0.03	0.01
Mg/Fe + Mg	0.48	0.48	0.48	0.47	0.52	0.49	0.49	0.51
Fe ³⁺ /Fe ³⁺ + Fe ²⁺	0.24	0.3	0.23	0.2	0.2	0.25	0.25	0.29
Fe ³⁺	0.31	0.4	0.31	0.26	0.24	0.32	0.33	0.37
Fe ²⁺	0.99	0.92	1.01	1.06	0.98	0.96	0.97	0.89
Mg	1.21	1.23	1.21	1.18	1.29	1.25	1.24	1.29
Fe ³⁺ %	0.12	0.16	0.12	0.1	0.09	0.13	0.13	0.14

(continued on next page)

Table 2 (continued)

Samples	Baiguoshu							
	w35b1	w33b1	w31b1	w21b1	w22b1	w24b1	w12b1	w13b1
Fe ²⁺ %	0.4	0.36	0.4	0.43	0.39	0.38	0.38	0.35
Mg%	0.48	0.48	0.48	0.47	0.52	0.49	0.49	0.51
2Fe ²⁺ + 3Fe ³⁺	2.91	3.03	2.94	2.91	2.66	2.9	2.94	2.9
Fe ²⁺ + Fe ³⁺	1.3	1.32	1.32	1.32	1.21	1.29	1.3	1.26
Mg =	1.21	1.23	1.21	1.18	1.29	1.25	1.24	1.29
Al ^{VI} + Fe ³⁺ + Ti	0.56	0.62	0.54	0.52	0.51	0.55	0.57	0.59
Fe ²⁺ + Mn	1.01	0.94	1.03	1.08	0.99	0.98	0.99	0.91
Sum	2.78	2.78	2.79	2.78	2.79	2.78	2.79	2.79
Mg%	0.43	0.44	0.44	0.42	0.46	0.45	0.44	0.46
(Al ^{VI} + Fe ³⁺ + Ti)%	0.2	0.22	0.2	0.19	0.18	0.2	0.2	0.21
(Fe ²⁺ + Mn)%	0.36	0.34	0.37	0.39	0.36	0.35	0.35	0.33

for all elements with counting times of 10 s and 5 s. The following standards were used: Sanidine (K), Pyrope Garnet (Fe), Diopside (Ca), Jadeite (Na), Diopside (Mg) and Pyrope Garnet (Al), Rhodonite (Mn), Olivine (Si), Rutile (Ti).

5. Results

5.1. Biotite

The Baiguoshu biotites show lower SiO₂ of 35.08–36.95 wt% than the Jilongshan samples (36.39–39.13 wt%), but both of them have similar Al₂O₃ contents of 14.09–15.46 wt% and 14.38–14.90 wt%, and similar MnO contents of 0.22–0.32 wt% and 0.24–0.32 wt% (Table 2). The Baiguoshu biotites contain higher FeO (19.33–20.92 wt%) but lower MgO (10.36–11.65 wt%) than the Jilongshan samples (10.35–17.07 wt% and 13.54–17.26 wt% respectively).

In this study, we apply the normalization of biotite compositions on the basis of 7 octahedral and tetrahedral cations which results in the calculated total positive charge that exceeds the theoretical maximum of 22 which assumes an anion framework of 10 oxygen and 2 (OH + F + Cl). The formula of this iterative normalization procedure for Jilongshan and Baiguoshu biotites is as follows: [Total Cations-(K + Na + Ca + Ba) + Ti + 1/2Al_{Xc}^{VI} = 7.0, where Al_{Xc}^{VI} = (Al + Cr)^{VI} - Al^{IV} + (K + Na + 2Ca + 2Ba)], which allocates a vacancy for each Ti and 2 Al_{Xc}^{VI}. This iterative normalization eliminates excess charge, and permits Fe³⁺ to be estimated (exclusive of oxyannite). On the mica classification diagram (Foster, 1960), all of the micas plotted in the magnesian biotite field (Fig. 7).

5.2. Amphibole

The Jilongshan amphiboles show higher SiO₂ contents (43.6–52.3 wt%) but lower Al₂O₃ (< 10.5 wt%) than the Baiguoshu ones (40.6–45.6 wt% and 10.3–12.3 wt%, respectively) (Table 3). Higher MgO (11.1–21.6 wt%) and lower FeO (3.6–16.6 wt%) are also observed for the Jilongshan amphiboles compared to the Baiguoshu samples which have lower MgO (8.9–13.3 wt%) but higher FeO (14.0 to 19.5 wt%). Both the Jilongshan and Baiguoshu amphiboles show very high CaO (> 10.5 wt%).

The normalization method of Leake et al. (1997) have been used to classify the amphiboles, and the following rules are applied (a) the formula is based on 24 (O, OH, F, Cl) if the H₂O and halogen contents are established (b) otherwise it will be calculated based on 23 (O) with 2 (OH, F, Cl) supposed, if cannot satisfy the criteria, an appropriate change of (OH + F + Cl) should be made. (c) Sum T to 8.00 using Si, then Al, then Ti. For the sake of simplicity of nomenclature, Fe³⁺ is not allocated to T. The normal maximum substitution for Si is 2, but this can be exceeded. (d) Sum C to 5.00 using excess Al and Ti from (c), and then successively Zr, Cr³⁺, Fe³⁺, Mn³⁺, Mg²⁺, Fe²⁺, Mn²⁺, any other L²⁺-type ions, and then Li. (e) Sum B to 2.00 using excess Mg²⁺,

Fe²⁺, Mn²⁺ and Li from (d), then Ca, then Na. (f) Excess Na from (e) is assigned to A, then all K. Total A should be between 0 and 1.00.

The amphiboles of Baiguoshu and Jilongshan plutons belong to the calcic group (Leake et al., 1997). The Jilongshan amphiboles show more Si and ferromagnesian than the Baiguoshu amphiboles. The Jilongshan amphiboles are dominated by the magnesiohornblende [□Ca₂[Mg₄(Al,Fe³⁺)Si₇AlO₂₂(OH)₂] and minor tremolite, actinolite and tschermakite, whilst the Baiguoshu samples are mainly the tschermakite [□Ca₂(Mg₃AlFe³⁺)Si₆Al₂O₂₂(OH)₂] and trace magnesiohornblende (Fig. 8).

5.3. Plagioclase

The plagioclases from Jilongshan show SiO₂ contents of 58.7–66.3 wt%, whereas the Baiguoshu plagioclases have SiO₂ contents of 51.5–60.6 wt% (Table 4). The Jilongshan plagioclases are characterized by 6.0–8.5 wt% CaO, 6.3–10.6 wt% Na₂O, and 24.3–26.3 wt % Al₂O₃. The Baiguoshu plagioclases have 24.6–25.9 wt% Al₂O₃, 6.3–8.2 wt% CaO, and 6.4–7.4 wt% Na₂O. The geochemical statistic calculation software (Geokit) has been used to normalize the plagioclase data based on 8 cations. The plagioclases in Jilongshan and Baiguoshu all belong to the andesine (Fig. 9).

6. Discussion

6.1. Estimation of temperature and pressure

The mineral chemistry of amphibole and feldspar has been widely used to constrain the temperature and pressure during the magma crystallization (Blundy and Holland, 1990, 1992; Anderson and Smith, 1995; Ridolfi et al., 2010; Aysal, 2015). As pointed out by many previous researchers, only the magma that emplaced into shallow crustal levels (mostly 1–2 kb or 3–6 km) may have the greatest potential to form economic porphyry deposits (e.g., Muntean and Einaudi, 2000; Xu et al., 2013). At shallow level, the volatile can be readily exsolved from the magma which is critical to the formation of magmatic-hydrothermal deposits, and the metals can be partitioned from melt into the exsolved hydrothermal fluids (e.g., Candela and Holland, 1984; Cline and Bodnar, 1991; Pokrovski et al., 2008). In particular, the Cu-poor porphyry Au deposits are characteristically emplaced at shallow crustal depths (Muntean and Einaudi, 2000).

In this study, the crystallization temperature and pressure are determined using the coexisting amphibole-plagioclase electron microprobe data (Table 5) by the relation: edenite + 4 quartz = tremolite + albite. The reaction edenite-tremolite exchange can carry out the temperature of crystallization with resolving several equations. The condition of thermometer application is T in the range 400–900 °C, amphiboles which have Na > 0.02 pfu, Al^{VI} < 1.8 pfu, and Si in the range 6.0–7.7, and plagioclases with X_{An} < 0.90. This approach does allow derivation of a thermometer which considers non-ideal

Table 3

Electron microprobe analyses and structural formula of amphibole from the Jilongshan and Baiguoshu granodiorites porphyry (wt%).

Samples	Jilongshan											
	z52h2	z52h1	z52h2	z53h1	z54h1	z55h1	z55h2	z103h1	z41h2	z42h1	z42h2	z43h1
SiO ₂	51.05	49.36	50.55	49.94	45.14	49.72	51.84	57.47	51.27	50.06	51.16	50.85
TiO ₂	0.6	0.94	0.83	0.74	1.17	0.99	0.52	0.21	0.75	0.99	0.74	0.82
Al ₂ O ₃	4.77	5.48	5.14	5.22	9.67	5.92	4.09	2.24	5.47	5.61	5.29	5.28
FeO	12.09	12.29	12.11	12.18	15.33	12.64	11.23	3.62	11.75	12.14	12.08	12.23
MnO	0.61	0.62	0.7	0.67	0.55	0.52	0.54	0.41	0.52	0.7	0.62	0.68
MgO	16.09	15.44	15.65	15.42	12.31	15.57	16.08	21.56	16.35	15.9	15.86	15.86
CaO	11.66	11.7	11.54	11.89	11.38	11.72	11.93	13.1	11.45	11.69	11.78	11.66
Na ₂ O	0.98	1.06	1.07	0.96	1.59	1.22	0.87	0.2	0.8	1.21	0.99	1.04
K ₂ O	0.4	0.53	0.49	0.45	0.98	0.54	0.34	0.12	0.36	0.53	0.44	0.45
Total	98.25	97.43	98.08	97.48	98.13	98.83	97.44	98.92	98.73	98.81	98.96	98.87
Si	7.29	7.15	7.25	7.23	6.64	7.11	7.45	7.82	7.26	7.14	7.26	7.23
Al ^{IV}	0.71	0.85	0.75	0.77	1.36	0.89	0.55	0.18	0.74	0.86	0.74	0.77
Sum T	8	8	8	8	8	8	8	8	8	8	8	8
Al ^{VI}	0.1	0.09	0.12	0.12	0.32	0.1	0.14	0.18	0.17	0.08	0.15	0.12
Ti	0.06	0.1	0.09	0.08	0.13	0.11	0.06	0.02	0.08	0.11	0.08	0.09
Fe ³⁺	0.36	0.33	0.33	0.29	0.35	0.35	0.2	−0.01	0.34	0.36	0.32	0.35
Mg	3.43	3.34	3.35	3.33	2.7	3.32	3.44	4.37	3.45	3.38	3.36	3.36
Fe ²⁺	1.05	1.14	1.12	1.19	1.5	1.12	1.15	0.42	0.96	1.07	1.1	1.08
Mn	0	0	0	0	0	0	0.01	0.01	0	0	0	0
Sum C	5	5	5	5	5	5	5	5	5	5	5	5
Mg	0	0	0	0	0	0	0	0	0	0	0	0
Fe ²⁺	0.03	0.02	0.01	0	0.03	0.04	0	0	0.09	0.02	0.02	0.02
Mn	0.07	0.08	0.08	0.08	0.07	0.06	0.06	0.03	0.06	0.08	0.07	0.08
Ca	1.78	1.82	1.77	1.84	1.79	1.8	1.84	1.91	1.74	1.79	1.79	1.78
Na	0.11	0.09	0.13	0.07	0.1	0.1	0.11	0.05	0.11	0.11	0.12	0.12
Sum B	2	2	2	2	2	2	2	2	2	2	2	2
Na	0.16	0.21	0.17	0.2	0.35	0.23	0.14	0	0.11	0.22	0.15	0.16
K	0.07	0.1	0.09	0.08	0.18	0.1	0.06	0.02	0.07	0.1	0.08	0.08
Sum A	0.23	0.31	0.25	0.28	0.53	0.33	0.2	0.02	0.18	0.32	0.23	0.25
Total	15.23	15.31	15.25	15.28	15.53	15.33	15.2	15.02	15.18	15.32	15.23	15.25
(Na + Ca)B	1.9	1.91	1.91	1.92	1.9	1.9	1.94	1.97	1.84	1.9	1.91	1.9
Mg/(Mg + Fe ²⁺)	0.76	0.74	0.75	0.74	0.64	0.74	0.75	0.91	0.77	0.76	0.75	0.75

Samples	Baiguoshu															
	w36h1	w35h1	w34h1	w34h2	w33h1	w32h1	w32h2	w31h1	w21h1	w22h1	w23h1	w24h1	w11h1	w12h1	w13h1	w14h1
SiO ₂	42.48	42.4	43.78	42.38	42.53	42.06	41.45	40.62	43.04	42.36	43.37	41.95	45.57	42.83	42.67	41.26
TiO ₂	0.97	1.17	0.97	1.57	1.26	1.26	1.24	1.23	1.07	1.75	1.44	1.26	0.9	1.53	1.24	1.39
Al ₂ O ₃	10.61	10.71	10.11	11.77	10.39	10.73	11.39	11.6	11.07	12.86	12.29	11.64	9.81	11.13	11.43	11.61
Fe ₂ O ₃	0	0	0	0	0	0	0	0	0	0	0	0	0	0	0	0
FeO	18.81	17.52	18.41	13.95	18.19	17.59	19.1	19.49	18.82	15.97	12.36	19.26	14.04	18.48	18.94	19
MnO	0.49	0.49	0.43	0.3	0.47	0.51	0.52	0.48	0.43	0.41	0.14	0.42	0.32	0.46	0.47	0.47
MgO	9.98	10.12	10.24	12.49	10.13	10.13	9.1	9	9.37	10.31	14.01	9.16	13.03	9.73	9.38	8.8
CaO	11.27	11.26	11.28	11.19	11.35	11.23	11.07	11.27	11.24	10.6	11.54	11.39	11.31	11.28	10.94	11.16
Na ₂ O	1.42	1.61	1.59	1.98	1.59	1.62	1.67	1.56	1.52	2.22	2.16	1.67	1.62	1.54	1.62	1.7
K ₂ O	1.06	1.11	0.81	0.79	0.95	0.95	1.23	1.42	1.15	0.63	0.84	1.21	0.75	1.2	1.24	1.21
Total	97.09	96.38	97.62	96.43	96.84	96.07	96.75	96.67	97.7	97.1	98.16	97.97	97.34	98.17	97.9	96.62
Si	6.43	6.45	6.57	6.32	6.45	6.42	6.34	6.25	6.48	6.32	6.3	6.34	6.69	6.42	6.41	6.33
Al ^{IV}	1.57	1.55	1.43	1.68	1.55	1.58	1.66	1.75	1.52	1.68	1.7	1.66	1.31	1.58	1.59	1.67
Sum T	8	8	8	8	8	8	8	8	8	8	8	8	8	8	8	8
Al ^{VI}	0.33	0.38	0.35	0.39	0.31	0.35	0.39	0.35	0.45	0.57	0.4	0.41	0.39	0.38	0.44	0.42
Ti	0.11	0.13	0.11	0.18	0.14	0.14	0.14	0.14	0.12	0.2	0.16	0.14	0.1	0.17	0.14	0.16
Fe ³⁺	0.47	0.34	0.39	0.41	0.39	0.38	0.4	0.42	0.34	0.36	0.4	0.35	0.36	0.35	0.41	0.33
Mg	2.25	2.3	2.29	2.78	2.29	2.3	2.07	2.06	2.1	2.29	3.03	2.06	2.85	2.17	2.1	2.01
Fe ²⁺	1.84	1.85	1.86	1.25	1.87	1.82	2	2.02	1.99	1.57	1.01	2.03	1.3	1.92	1.92	2.07
Mn	0	0	0	0	0	0	0	0	0	0	0	0	0	0	0	0
Sum C	5	5	5	5	5	5	5	5	5	5	5	5	5	5	5	5
Mg	0	0	0	0	0	0	0	0	0	0	0	0	0	0	0	0
Fe ²⁺	0.07	0.04	0.06	0.08	0.05	0.04	0.05	0.06	0.04	0.05	0.1	0.05	0.06	0.04	0.06	0.03
Mn	0.06	0.06	0.05	0.04	0.06	0.07	0.07	0.06	0.05	0.05	0.02	0.05	0.04	0.06	0.06	0.06
Ca	1.83	1.84	1.81	1.79	1.84	1.84	1.81	1.86	1.81	1.69	1.8	1.84	1.78	1.81	1.76	1.83
Na	0.04	0.06	0.07	0.09	0.04	0.05	0.07	0.02	0.09	0.2	0.09	0.06	0.12	0.09	0.12	0.07
Sum B	2	2	2	2	2	2	2	2	2	2	2	2	2	2	2	2
Na	0.38	0.41	0.39	0.48	0.42	0.43	0.42	0.44	0.36	0.44	0.52	0.43	0.34	0.36	0.35	0.43
K	0.2	0.22	0.15	0.15	0.18	0.18	0.24	0.28	0.22	0.12	0.16	0.23	0.14	0.23	0.24	0.24
Sum A	0.58	0.63	0.54	0.63	0.61	0.61	0.66	0.72	0.58	0.56	0.67	0.67	0.48	0.59	0.59	0.67
Total	15.58	15.63	15.54	15.63	15.61	15.61	15.66	15.72	15.58	15.56	15.67	15.67	15.48	15.59	15.59	15.67
(Na + Ca)B	1.86	1.9	1.89	1.88	1.89	1.89	1.88	1.9	1.9	1.9	1.9	1.9	1.9	1.88	1.88	1.91
Mg/(Mg + Fe ²⁺)	0.54	0.55	0.54	0.68	0.54	0.55	0.5	0.51	0.58	0.73	0.5	0.68	0.53	0.52	0.49	

Table 4

Electron microprobe analyses and structural formula of feldspar from the Jilongshan and Baiguoshu granodiorites porphyry (wt%).

Samples	Jilongshan													
	z52p1	z52p1	z52p2	z53p1	z54p1	z55p1	z103p1	z101p1	z101p2	z102p1	z42p1	z43p1	z44p1	z45p1
SiO ₂	59.26	60.47	59.52	66.34	59.72	58.76	60.12	58.61	58.85	61.68	61.17	60.71	61.58	61.08
Al ₂ O ₃	25.92	24.97	25.52	20.58	24.84	25.25	25.43	26.48	26.26	24.51	24.64	25.09	24.59	24.77
CaO	7.86	6.72	7.16	1.53	6.64	7.5	7.47	8.5	8.32	6.19	6.51	6.98	6.24	6.55
Na ₂ O	6.68	7.34	7.17	10.61	7.17	6.74	6.63	6.36	6.64	7.37	7.21	6.99	7.31	6.34
K ₂ O	0.39	0.59	0.47	0.12	0.7	0.61	0.54	0.37	0.42	0.61	0.67	0.72	0.89	0.78
Total	100.1	100.1	99.84	99.18	99.07	98.86	100.2	100.3	100.5	100.4	100.2	100.5	100.6	99.52
Si	2.64	2.69	2.66	2.93	2.69	2.65	2.67	2.61	2.62	2.73	2.71	2.69	2.72	2.72
Al	1.36	1.31	1.34	1.07	1.32	1.34	1.33	1.39	1.38	1.28	1.29	1.31	1.28	1.3
Ca	0.38	0.32	0.34	0.07	0.32	0.36	0.36	0.41	0.4	0.29	0.31	0.33	0.3	0.31
Na	0.58	0.63	0.62	0.91	0.63	0.59	0.57	0.55	0.57	0.63	0.62	0.6	0.63	0.55
K	0.02	0.03	0.03	0.01	0.04	0.03	0.03	0.02	0.02	0.03	0.04	0.04	0.05	0.04
An	38.53	32.44	34.62	7.33	32.48	36.74	37.16	41.59	39.94	30.57	31.98	34.07	30.41	34.57
Ab	59.2	64.15	62.66	91.99	63.43	59.72	59.64	56.28	57.65	65.87	64.09	61.76	64.41	60.52
Or	2.27	3.41	2.73	0.68	4.09	3.54	3.20	2.13	2.42	3.56	3.93	4.17	5.18	4.91

Samples	Baiguoshu												
	w362	w351	w341	w342	w331	w321	w221	w231	w241	w111	w121	w131	w141
SiO ₂	60.58	59.03	59.03	59.43	59.16	57.52	59.75	58.18	59.71	60.65	60.11	59.71	59.88
Al ₂ O ₃	24.58	24.9	24.95	24.78	24.94	25.93	24.99	25.97	25.1	24.6	25.28	25.38	25.34
CaO	6.31	6.84	6.94	6.48	6.77	8.01	7.13	8.24	6.99	6.62	7.12	7.49	7.04
Na ₂ O	7.39	7.29	7.13	7.45	7.11	6.52	6.87	6.44	7.14	7.24	6.9	6.78	6.93
K ₂ O	0.58	0.49	0.51	0.58	0.54	0.44	0.5	0.41	0.51	0.57	0.49	0.46	0.54
Total	99.44	98.55	98.56	98.72	98.52	98.42	99.24	99.45	99.68	99.9	99.82	99.73	
Si	2.71	2.67	2.67	2.68	2.68	2.61	2.68	2.62	2.68	2.71	2.68	2.67	2.67
Al	1.3	1.33	1.33	1.32	1.33	1.39	1.32	1.38	1.33	1.29	1.33	1.34	1.33
Ca	0.3	0.33	0.34	0.31	0.33	0.39	0.34	0.4	0.34	0.32	0.34	0.36	0.34
Na	0.64	0.64	0.63	0.65	0.62	0.57	0.6	0.56	0.62	0.63	0.6	0.59	0.6
K	0.03	0.03	0.03	0.03	0.03	0.03	0.03	0.02	0.03	0.03	0.03	0.03	0.03
An	30.98	33.16	33.94	31.38	33.38	39.39	35.39	40.42	34.08	32.45	35.28	36.9	34.81
Ab	65.62	64.01	63.08	65.27	63.43	58.03	61.67	57.17	62.98	64.21	61.85	60.38	62.0
Or	3.4	2.84	2.99	3.34	3.19	2.58	2.94	2.41	2.94	3.34	2.88	2.72	3.18

interactions within a compositionally complex phase (amphibole) and hence a thermometer which is applicable to a wide range in bulk composition. The amphibole multi-site solid solution is complex, and we used the simple (symmetrical) form of non-ideal interactions of Holland and Blundy (1994) that involves the distribution of the species Y-K-Na-Ca-Mg-Fe²⁺-Fe³⁺-AlSi over the A, M4, M1, M3, M2 and T1 crystallographic sites. The temperature calculation formula is as following:

$$T = \frac{\Delta H^0 + P\Delta V^0 + Y_{ab} + Y_{ed-tr}}{\Delta S^0 - R \ln K_{ideal}^{ed-tr}}$$

$$P(\pm 0.6 \text{ kbar}) = 4.76\text{Al} - 3.01 - \{[T(\text{ }^\circ\text{C}) - 675]/85] \\ \times \{0.530\text{Al} + 0.005294[T(\text{ }^\circ\text{C}) - 675]\}.$$

$$T = \frac{-76.95 + 0.79P + Y_{ab} + 39.4X_{Na}^A + 22.4X_K^A + (41.5 - 2.89P) \cdot X_{Al}^{M2}}{-0.0650 - R \cdot \ln \left(\frac{27 \cdot X_{Na}^A \cdot X_{Si}^T \cdot X_{ab}^{plag}}{256 \cdot X_{Na}^A \cdot X_{Al}^T} \right)}$$

The Y_{ab} term is given by: for X_{ab} > 0.5 then Y_{ab} = 0, otherwise Y_{ab} = 12.0(1 - X_{ab})² - 3.0 kJ. T is the temperature in Kelvins, P is the pressure in kbar and the X_i^φ terms denote the molar fraction of species (or component) in phase (or crystallographic site) φ. The values of Y_{ab} depend upon the plagioclase composition and the components which make up Y_(ed-tr) must be determined, along with ΔH⁰ and ΔS⁰ by regression of the data. We used the imposed literature value of 0.79 kJ kbar⁻¹ for ΔV⁰ in subsequent regressions (Holland and Blundy, 1994). Pressure correlates with temperature ($r^2 = 0.86$), indicating that temperature-sensitive edenite exchange has a considerable influence on pressure variations (Holland and Blundy, 1994). The edenite-forming

reaction: albite + tremolite to quartz + edenite, using the exchange mechanism Si + Y_A + Al^{IV} + (K + Na)_A affect Al in hornblende. Additional important variables include temperature-sensitive substitutions involving Ti, with Ti + R²⁺ = 2Al^{VI} and Ti + Al^{VI} = Al^{VI} + Si, and fO₂-controlled Fe²⁺-Fe³⁺ variations allow the operation of the exchange vector Fe³⁺ = Al^{VI} (Anderson and Smith, 1995). We have used many thermometers with similar results, and this one shows the most acceptable results of temperature and pressure proved by the previous investigation in the Jiurui district.

The Baiguoshu crystallization temperature and pressure are higher (724 to 832 °C, 3.2 to 6.3 kbar) than the Jilongshan (624 to 736 °C, 0.4 to 0.9 kbar) (Fig. 10). These temperatures are similar to those estimated from zircon thermometers (744–752 °C and 634–824 °C) (Pang et al., 2014).

6.2. Estimation of oxygen fugacity

There are a number of ways to estimate the oxygen fugacity of a magma, including whole-rock chemical ratios such as Fe³⁺/Fe²⁺ ratios (Blevin, 2004), rare earth elements (Eu and Ce anomaly) in whole-rocks or minerals such as zircon (Ballard et al., 2002; Burnham and Berry, 2014), and mineral equilibria using electron microprobe analyses of a number of silicate minerals such as amphibole and biotite (Zhao et al., 2005; Ridolfi et al., 2010).

In this study, the oxygen fugacity has been calculated by the biotite compositional data. The oxygen fugacity estimation from zircon trace elements and from amphibole estimated by the method of Ridolfi et al. (2010) (Table 6) confirmed the obtained results from biotite chemistry. A significant change in X_{Mg} between biotites in different intrusions is observed. The calculated Fe³⁺/Fe²⁺ ratios for the Jilongshan biotites

Table 5

The structural formula of coexisting amphibole-plagioclase and the calculated results for temperature (°C) and pressure (kbar).

Jilongshan												Baiguoshu					
Amphibole	z21	z221	z241	z521	z522	z461	w321	w341	w342	w111	w141	w221	w231	w241			
Cations on the basis of 13 cations																	
Si																	
Si	7.382	7.196	7.224	7.102	7.199	7.417	5.352	6.508	6.263	6.638	6.281	6.265	6.246	6.288			
Ti	0.06	0.09	0.11	0.1	0.09	0.06	0.41	0.11	0.17	0.1	0.16	0.19	0.16	0.14			
Al	0.72	0.84	0.85	0.93	0.86	0.71	2.3	1.77	2.05	1.68	2.08	2.24	2.09	2.06			
Cr	0	0	0	0	0	0	0	0	0	0	0	0	0	0	0	0	0
Fe	1.4	1.47	1.46	1.48	1.44	1.38	2.03	2.29	1.72	1.71	2.42	1.97	1.49	2.41			
Mn	0.08	0.06	0.07	0.08	0.08	0.08	0.03	0.05	0.04	0.04	0.06	0.05	0.02	0.05			
Mg	3.36	3.34	3.29	3.31	3.32	3.36	2.88	2.27	2.75	2.83	2	2.27	3.01	2.05			
Ca	1.8	1.83	1.8	1.8	1.76	1.8	0.01	1.8	1.77	1.77	1.82	1.68	1.78	1.83			
Na	0.23	0.3	0.32	0.3	0.3	0.23	0.03	0.46	0.57	0.46	0.5	0.64	0.6	0.49			
K	0.06	0.08	0.09	0.1	0.09	0.06	1.78	0.15	0.15	0.14	0.24	0.12	0.15	0.23			
Ti(IV)	0	0	0	0	0	0	0.35	0	0	0	0	0	0	0	0	0	0
Ti(VI)	0.06	0.09	0.11	0.1	0.09	0.06	0.06	0.11	0.17	0.1	0.16	0.19	0.16	0.14			
Al(IV)	0.62	0.8	0.78	0.9	0.8	0.58	2.3	1.49	1.74	1.36	1.72	1.74	1.75	1.71			
Al(VI)	0.1	0.04	0.07	0.03	0.06	0.12	0	0.28	0.31	0.32	0.36	0.51	0.33	0.34			
Mg/Fe + Mg	0.71	0.69	0.69	0.69	0.7	0.71	0.59	0.5	0.61	0.62	0.45	0.54	0.67	0.46			
Fe ³⁺ /Fe ³⁺ + Fe ²⁺	0.36	0.37	0.32	0.45	0.46	0.33	2.15	0.34	0.47	0.42	0.27	0.37	0.53	0.29			
BCa	1.8	1.83	1.8	1.8	1.76	1.8	0.01	1.8	1.77	1.77	1.82	1.68	1.78	1.83			
BNa	0.2	0.17	0.2	0.2	0.24	0.2	0.03	0.2	0.23	0.23	0.18	0.32	0.22	0.17			
ANa	0.03	0.13	0.12	0.1	0.06	0.03	0	0.26	0.34	0.22	0.32	0.32	0.38	0.31			
A(empty)	0.91	0.79	0.79	0.8	0.86	0.91	1.19	0.59	0.51	0.64	0.44	0.57	0.46	0.45			
2Fe ²⁺ + 3Fe ³⁺	3.31	3.49	3.4	3.62	3.54	3.2	8.42	5.36	4.26	4.14	5.5	4.68	3.77	5.54			
Fe ²⁺ + Fe ³⁺	1.4	1.47	1.46	1.48	1.44	1.38	2.03	2.29	1.72	1.71	2.42	1.97	1.49	2.41			
Fe ³⁺	0.51	0.55	0.47	0.66	0.66	0.45	4.36	0.79	0.82	0.72	0.66	0.73	0.79	0.71			
Fe ²⁺	0.89	0.92	0.99	0.82	0.79	0.92	-2.33	1.5	0.91	0.99	1.76	1.25	0.7	1.7			
Plagioclase	z21	z221	z241	z521	z522	z461	w321	w341	w342	w111	w141	w221	w231	w241			
Cations on the basis of 8 oxygens																	
Si	2.67	2.68	2.73	2.69	2.66	2.68	2.61	2.67	2.68	2.7	2.67	2.68	2.62	2.67			
Al	1.32	1.32	1.27	1.31	1.34	1.31	1.39	1.33	1.32	1.29	1.33	1.32	1.38	1.32			
Ca	0.35	0.33	0.29	0.32	0.34	0.32	0.39	0.34	0.31	0.32	0.34	0.34	0.4	0.34			
Na	0.59	0.63	0.63	0.63	0.62	0.64	0.57	0.63	0.65	0.63	0.6	0.6	0.56	0.62			
K	0.04	0.03	0.05	0.03	0.03	0.03	0.03	0.03	0.03	0.03	0.03	0.03	0.02	0.03			
Fe	0.01	0.01	0.01	0.01	0.01	0.01	0.01	0	0.01	0.01	0.01	0.01	0.01	0.01			
Ca + Na + K	0.98	0.98	0.97	0.99	0.99	0.99	0.99	0.99	0.99	1	0.97	0.97	0.97	0.98	0.98		
XAn(Ca)	0.36	0.33	0.3	0.32	0.35	0.33	0.39	0.34	0.31	0.32	0.35	0.35	0.4	0.34			
XAb(Na)	0.6	0.64	0.65	0.64	0.63	0.64	0.58	0.63	0.65	0.64	0.62	0.62	0.57	0.63			
XOr(K)	0.04	0.03	0.05	0.03	0.03	0.03	0.03	0.03	0.03	0.03	0.03	0.03	0.02	0.03			
Temperature	648	730	704	736	697	624	816	767	798	724	785	748	832	787			
Pressure	0.5	0.5	0.8	0.8	0.9	0.4	3.2	3.9	4.2	4.4	4.7	6.3	3.3	4.6			

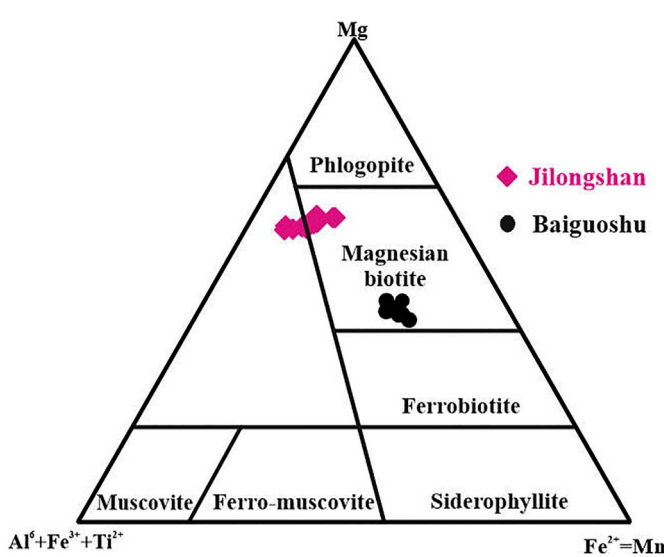


Fig. 7. Ternary classification diagram of biotite from the Jilongshan and Baiguoshu plutons.
(modified after Foster, 1960)

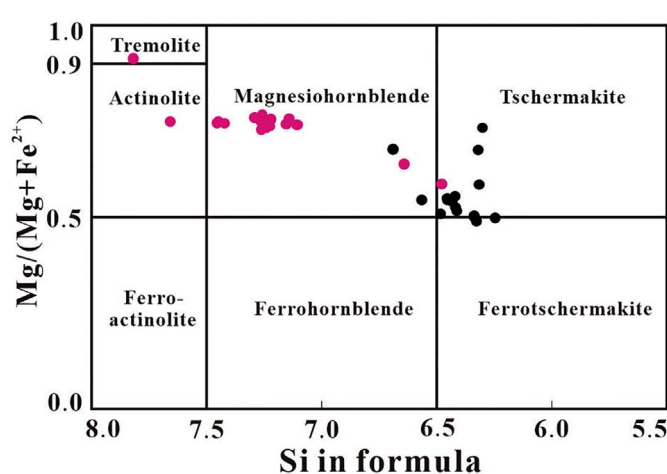


Fig. 8. Classification of the calcic amphiboles from the Jilongshan and Baiguoshu plutons.
(modified after Leake et al., 1997)

are obviously higher than those of Baiguoshu ones. The Fe³⁺ and Fe²⁺ contents of biotite could indicate the fO₂ conditions when they formed (Zhao et al., 2005). The results show that the Jilongshan biotites have higher contents of Fe³⁺, which suggests that they may have formed

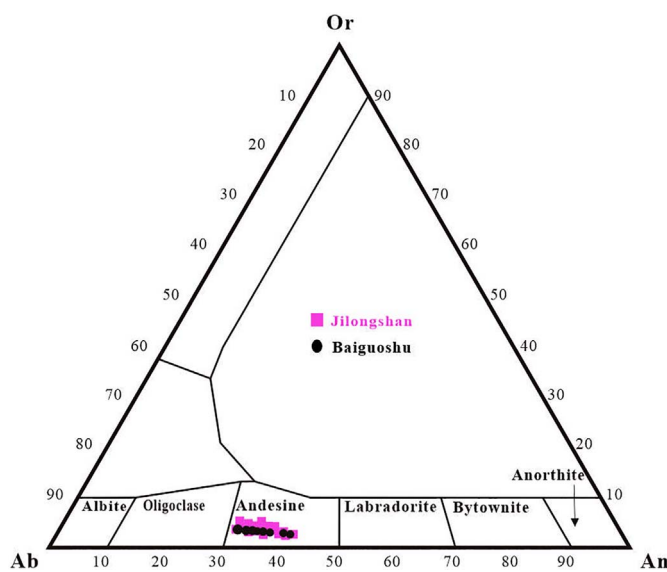


Fig. 9. Ternary classification of plagioclases from the Jilongshan and Baiguoshu plutons. (modified after Deer et al., 1992)

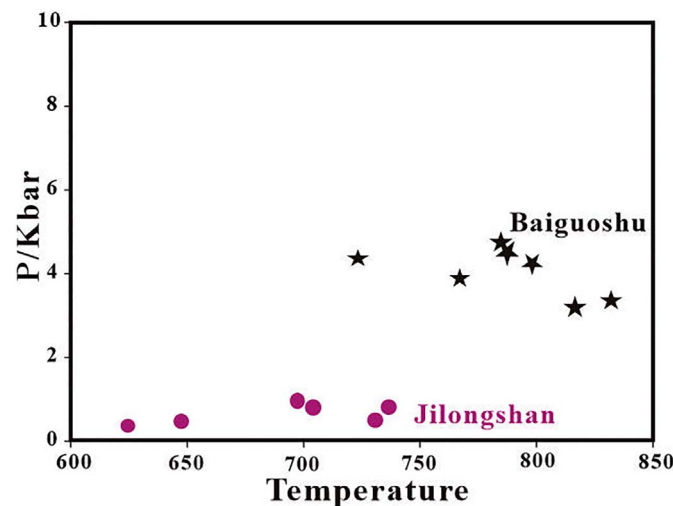


Fig. 10. Plot of temperature and pressure of the Jilongshan and Baiguoshu plutons.

under relatively more oxidizing conditions and half of the data plots above the HM buffer line whereas all the data from the Baigoushu biotites plots below the HM buffer line (Fig. 11). Therefore, we suggest that the magma responsible for the Jilongshan pluton was rich in Mg and had a higher oxygen fugacity than the Baigoushu.

6.3. Implication for mineral prospecting

In the Jurui district, a large number of intrusions are presented, but only some with mineralization and many are barren. Hence, it is important to set up a criterion to distinguish between the ore-related and the barren plutons.

The Baigoushu magma crystallization temperature ($724\text{--}832^{\circ}\text{C}$) represents the highest of this study with average pressure at around 4 kbar. The magma crystallization temperature of Jilongshan ($624\text{--}736^{\circ}\text{C}$) is lower than the Baigoushu, and the lower pressure of the Jilongshan pluton (0.4–0.9 kbar) is similar to those ore-bearing plutons in the Jurui district as previously suggested by Xu et al. (2013). For example, the ore-bearing granodiorite porphyry in the Wushan and Donglewan Cu–Au deposits show larger temperature range of

$665\text{--}832^{\circ}\text{C}$ and $644\text{--}855^{\circ}\text{C}$ and very low crystallization pressure of 0–2.7 kbar and 0.1–1.8 kbar, respectively (Xu et al., 2013). Xu et al. (2013) concluded that the intrusive rocks with pressure higher than 4 kbar in the Jurui district are generally characterized by low mineralization potential but those emplaced at shallow crustal levels (average 1.4 kbar) are generally associated with economic Cu–Au mineralization. Cline and Bodnar (1991) also pointed out that a magma with an initial composition of 2.5 wt% H_2O , $\text{Cl}/\text{H}_2\text{O} = 0.1$, and 50 ppm Cu, could generate an economic porphyry deposit if emplaced at a shallow crustal depth (~ 2 kbar), and the larger the volumes of magma, the larger the mineral deposits potential. Pirajno (2009) also pointed out that skarn type mineralization is more favorable at 0.3–3 kbar, which is similar to those Cu–Au deposits in the Jurui district.

Therefore, it is suggested that the Baigoushu pluton may have less potential for Au–Cu mineralization. In contrast, the Jilongshan pluton has great potential and is more prospective. Therefore, deep exploration in the Jilongshan pluton should be carried out in the future.

The role of the oxygen fugacity of magma is fundamentally important for porphyry and skarn type Au–Cu mineralization (Ballard et al., 2002; Sillitoe, 2010; Richards, 2015). At relatively higher oxygen fugacity, the sulfur in the melt will remain as $\text{S}^{6+}(\text{SO}_4^{2-})$ rather than S^{2-} , and therefore prevent formation of sulfide melt or sulfide minerals at the deep magma chamber, which give immense potential for the metals to be carried out to shallow crystallization site to form economic porphyry deposits (Nilsson and Peach, 1993; Métrich and Clocchiatti, 1996; Sun et al., 2004; Richards, 2015). The high $f\text{O}_2$ can facilitate the destabilization of mantle sulfides to release Cu–Au that are hosted in sulfides, and contribute to the later enrichment of Cu–Au in the magmas (Liu et al., 2010).

The $f\text{O}_2$ of the Jilongshan intrusive rocks has a wider variation range with half of the data plot above the HM buffer line than the Baigoushu pluton that all plot below the HM buffer line. Previous studies in the Jurui district have suggested that higher $f\text{O}_2$ (higher than HM buffer line) is beneficial to Cu–Au mineralization (Xu et al., 2013). Therefore, the oxygen fugacity conditions also indicate the Jilongshan pluton has greater potential for further deep-exploration than the Baigoushu pluton which show less potential for major mineralization.

7. Conclusions

This study presents in detail the principal characteristics of biotite, amphibole and plagioclase in the Jilongshan ore-bearing granodiorite porphyry and the Baigoushu pluton which is adjacent to the Jilongshan Au–Cu deposit but until now the investigations show that there is no mineralization. The following conclusions can be drawn:

- 1) The biotites of the investigated plutons all belong to the magnesian biotite, but the Baigoushu is richer in Fe^{2+} and Mn. The Baigoushu and Jilongshan contain calcic amphibole but the Baigoushu with low Si present mainly tschermakite and the Jilongshan accommodate principally the magnesiohornblende. The plagioclases of Baigoushu and Jilongshan both consist of andesine.
- 2) The magma crystallization temperature and pressure are not the same in the studied plutons; the Jilongshan shows the lowest pressure and moderate temperature range, whereas the Baigoushu has higher temperature and higher pressure. The Jilongshan pluton shows a high oxygen fugacity than the Baigoushu. These data can permit us to surely conclude that the Jilongshan pluton show higher potential for mineralization and therefore deep-exploration should be further carried out in this region.

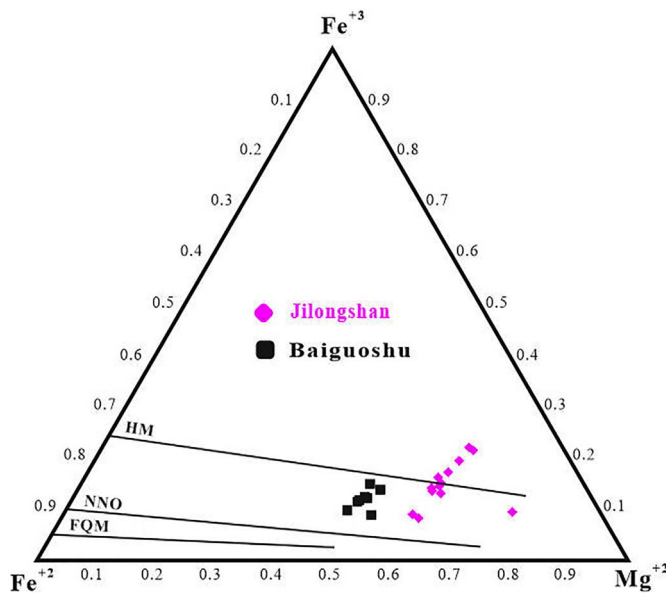
Acknowledgments

This study is financially supported by the National Key R & D Program of China (no. 2016YFC0600206) and the special fund from the State Key Laboratory of Geological Processes and Mineral Resources

Table 6A comparison of f_{O_2} the Jilongshan and Baiguoshu amphiboles.

Samples	Jilongshan																	
	Test	z52h2	z52h1	z52h2	z53h1	z54h1	z55h1	z55h2	z41h2	z42h1	z42h2	z43h1	z43h3	z46h1	z2h1	z22h2	z23h1	z24h1
ΔNNO	2.1	2.2	1.9	2.0	2.0	0.8	1.9	2.2	2.2	2.0	2.0	2.1	2.0	2.1	2.1	2.0	0.3	1.8
$\log f_{O_2}$	-12.8	-13.0	-12.6	-13.0	-12.8	-11.8	-12.5	-13.5	-12.5	-12.5	-12.9	-12.8	-12.7	-13.6	-13.5	-12.9	-11.8	-13.1
Uncertainty	0.4	0.4	0.4	0.4	0.4	0.4	0.4	0.4	0.4	0.4	0.4	0.4	0.4	0.4	0.4	0.4	0.4	0.4
T (°C)	757	742	770	751	759	862	777	723	762	772	751	754	759	719	723	756	886	753
Uncertainty	22	22	22	22	22	22	22	22	22	22	22	22	22	22	22	22	22	22
P (MPa)	66	60	73	66	69	210	80	52	70	74	68	68	67	53	54	64	261	65
Uncertainty (max error)	7	7	8	7	8	53	9	6	8	8	7	7	7	6	6	7	65	7

Samples	Baiguoshu														
	w36h1	w35h1	w34h1	w34h2	w33h1	w32h1	w32h2	w31h1	w21h1	w23h1	w24h1	w11h1	w12h1	w13h1	w14h1
ΔNNO	0.3	0.2	0.3	0.7	0.2	0.2	-0.1	-0.1	0.0	1.0	-0.2	1.1	0.0	0.0	-0.3
$\log f_{O_2}$	-11.9	-11.9	-12.3	-10.6	-12.0	-11.8	-11.9	-11.7	-12.3	-10.0	-11.9	-11.5	-12.1	-12.1	-12.0
Uncertainty	0.4	0.4	0.4	0.4	0.4	0.4	0.4	0.4	0.4	0.4	0.4	0.4	0.4	0.4	0.4
T (°C)	881	889	861	931	883	893	901	917	878	947	905	860	890	887	908
Uncertainty	22	22	22	22	22	22	22	22	22	22	22	22	22	22	22
P (MPa)	284	298	245	366	271	301	358	384	317	386	369	216	317	344	384
Uncertainty (max error)	71	74	61	40	68	75	89	96	79	42	92	54	79	86	96

Fig. 11. Plot of Fe^{3+} - Fe^{2+} -Mg of biotite from the Jilongshan and Baiguoshu plutons. (modified after Wones and Eugster, 1965)

(MSFGPMR03). We thank Dr. Yang Shuiyuan for his help with the EMPA analyses. Prof. A.W. Hofmann and Prof. Zhao Kuidong are thanked for their valuable discussion and suggestion for this work.

References

- Anderson, J.L., Smith, D.R., 1995. The effects of temperature and f_{O_2} on the Al-in-hornblende barometer. Am. Mineral. 80 (5–6), 549–559.
- Aysal, N., 2015. Mineral chemistry, crystallization conditions and geodynamic implications of the Oligo-Miocene granitoids in the Biga Peninsula, Northwest Turkey. J. Asian Earth Sci. 105, 68–84.
- Ballard, J.R., Michael Palin, J., Campbell, I.H., 2002. Relative oxidation states of magmas inferred from Ce(IV)/Ce(III) in zircon: application to porphyry copper deposits of northern Chile. Contrib. Mineral. Petrol. 144, 347–364.
- Bi, Z.M., Yang, S., 2008. Geological and mineral resources characteristics, metalsources and metallogenetic mechanism of Jilongshan skarn Au (Cu) deposit. Mineral Res. Geol. 22 (6), 496–502 (In Chinese with English abstract).
- Blevin, P.L., 2004. Redox and compositional parameters for interpreting the granitoid metallogenesis of Eastern Australia: implications for gold-rich ore system. Resour. Geol. 54, 241–252.
- Blundy, J.D., Holland, T.J.B., 1990. Calcic amphibole equilibria and a new amphibole-plagioclase geothermometer. Contrib. Mineral. Petrol. 104 (2), 208–224.
- Blundy, J.D., Holland, T.J.B., 1992. Calcic amphibole equilibria and a new amphibole-plagioclase geothermometer - reply to the comment of Poli and Schmidt. Contrib. Mineral. Petrol. 111, 278–282.
- Burnham, A.D., Berry, A.J., 2014. The effect of oxygen fugacity, melt composition, temperature and pressure on the oxidation state of cerium in silicate melts. Chem. Geol. 366, 52–60.
- Candela, P.A., Holland, H.D., 1984. The partitioning of copper and molybdenum between silicate melts and aqueous fluids. Geochim. Cosmochim. Acta 48, 373–380.
- Chang, Y.F., Liu, X.P., Wu, Y.C., 1991. The Copper-Iron Belt of the Lower and Middle Reaches of the Changjiang River. Geological Publishing House, Beijing, pp. 1–379 (in Chinese with English abstract).
- Cline, J.S., Bodnar, R.J., 1991. Can economic porphyry copper mineralization be generated by a typical calc-alkaline melt? J. Geophys. Res. 96, 8113–8126.
- Deer, W.A., Howie, R.A., Zussman, J., 1992. An Introduction to the Rock-Forming Minerals, 2nd Edition. Longman Group, Harlow, pp. 1–232.
- Ding, X., Jiang, S.Y., Ni, P., Gu, L.X., Jiang, Y.H., 2005. Zircon SIMS U-Pb geochronology of host granitoids in Wushan and Yongping copper deposits, Jiangxi Province. Geol. J. China Univ. 11, 383–389.
- Foster, M.D., 1960. Interpretation of the composition of trioctahedral micas. USGS Prof. Paper 354 (B), 1–146.
- Holland, T., Blundy, J., 1994. Non-ideal interactions in calcic amphiboles and their bearing on amphibole-plagioclase thermometry. Contrib. Mineral. Petrol. 116 (4), 433–447.
- Hu, J.P., Jiang, S.Y., 2010. Zircon U-Pb dating and Hf isotopic compositions of porphyries from the Ningwu Basin and their geological implications. Geol. J. China Univ. 16, 294–308 (in Chinese with English abstract).
- Jiang, S.Y., Li, L., Zhu, B., Ding, X., Jiang, Y.H., Gu, L.X., Ni, P., 2008. Geochemical and Sr-Nd-Hf isotopic compositions of granodiorite from the Wushan copper deposit, Jiangxi province and implication for petrogenesis. Acta Petrol. Sin. 24 (8), 1679–1690 (in Chinese with English abstract).
- Jiang, S.Y., Xu, R.M., Zhu, Z.Y., Zhou, W., Kong, F.B., Sun, Y., 2013. Study on Mesozoic tectonics and granitic magmatism and their relationship with Cu-Au mineralization in the Jiurui ore district, Jiangxi Province. Acta Petrol. Sin. 29 (12), 4051–4068.
- Khin, Z., Peters, S.G., Cromie, P., Burnett, C., Hou, Z., 2007. Nature, diversity of deposit types and metallogenetic relations of South China. Ore Geol. Rev. 31, 3–47.
- Leake, B.E., Woolley, A.R., Arps, C.E.S., Birch, W.D., Gilbert, M.C., Grice, J.D., Hawthorne, F.C., Kato, A., Kisch, H.J., Krivovichev, V.G., Linthout, K., Laird, J., Mandarino, J.A., Maresch, W.V., Nickel, E.H., Rock, N.M.S., Schumacher, J.C., Smith, D.C., Stephenson, N.C.N., Ungarotti, L., Whittaker, E.J.W., Guo, Y.Z., 1997. Nomenclature of amphiboles: report of the subcommittee on amphiboles of the international mineralogical association, commission on new minerals and mineral names. Am. Mineral. 82 (9–10), 1019–1037.
- Li, L., Jiang, S.Y., 2009. Petrogenesis and geochemistry of the Dengjiashan porphyritic granodiorite, Jiujiang Ruichang metallogenic district of the Middle Reaches of the Yangtze River. Acta Petrol. Sin. 25 (11), 2877–2888 (in Chinese with English abstract).
- Li, X.H., Li, W.X., Wang, X.C., Li, Q.L., Liu, Y., Tang, G.Q., 2010. SIMS U-Pb zircon

- geochronology of porphyry Cu–Au–(Mo) deposits in the Yangtze River Metallogenic Belt, eastern China: magmatic response to early Cretaceous lithospheric extension. *Lithos* 119, 427–438.
- Liu, S.A., Li, S.G., He, Y.S., Huang, F., 2010. Geochemical contrasts between early Cretaceous ore-bearing and ore-barren high-Mg adakites in central-eastern China: implications for petrogenesis and Cu–Au mineralization. *Geochim. Cosmochim. Acta* 74, 7160–7178.
- Mao, J.W., Wang, Y.T., Lehmann, B., Du, A.D., Mei, Y.X., Li, Y.F., Zang, W.S., Stein, H.J., Zhou, T.F., 2006. Molybdenite Re–Os and albite $^{40}\text{Ar}/^{39}\text{Ar}$ dating of Cu–Au–Mo and magnetite porphyry systems in the Yangtze River valley and metallogenic implications. *Ore Geol. Rev.* 29 (2006), 307–324.
- Métrich, N., Clocchiatti, R., 1996. Sulfur abundance and its speciation in oxidized alkaline melts. *Geochim. Cosmochim. Acta* 60, 4151–4160.
- Mo, H.Z., Wang, C.R., Chang, H.P., Zhu, Y.G., Xie, D.Q., Xiong, J.H., 2011. Succeed resource exploration geological report of Jilongshan gold deposit, Yangxin County, Hubei Province. In: Geological Exploration Institute of South China, pp. 1–10 (in Chinese).
- Muntean, J.L., Einaudi, M.T., 2000. Porphyry gold deposits of the Refugio district, Maricunga belt, northern Chile. *Econ. Geol.* 95, 1445–1472.
- Nilsson, K., Peach, C.L., 1993. Sulfur speciation, oxidation state, and sulfur concentration in backarc magmas. *Geochim. Cosmochim. Acta* 57, 3807–3813.
- Pan, Y.M., Dong, P., 1999. The Lower Changjiang (Yangzi/Yangtze River) metallogenic belt, east central China: intrusion - and wall rock-hosted Cu–Fe–Au, Mo, Zn, Pb, Ag deposits. *Ore Geol. Rev.* 15, 177–242.
- Pang, A.J., Sheng, R.L., Santosh, M., Qing, Y.Y., Bao, J.J., Cheng, D.Y., 2014. Geochemistry, and zircon U–Pb and molybdenite Re–Os geochronology of Jilongshan Cu–Au deposit, southeastern Hubei Province, China. *Geol. J.* 49, 52–68.
- Pirajno, F., 2009. Hydrothermal Processes and Mineral Systems. Springer, Berlin, pp. 1–1250.
- Pokrovski, G.S., Borisova, A.Y., Harrichoury, J.C., 2008. The effect of sulfur on vapor–liquid fractionation of metals in hydrothermal systems. *Earth Planet. Sci. Lett.* 266, 345–362.
- Richards, J.P., 2015. The oxidation state, and sulfur and Cu contents of arc magmas: implications for metallogeny. *Lithos* 233, 27–45.
- Ridolfi, F., Renzulli, A., Puerini, M., 2010. Stability and chemical equilibrium of amphibole in calc-alkaline magmas: an overview, new thermobarometric formulations and application to subduction-related volcanoes. *Contrib. Mineral. Petro.* 160, 45–66.
- Sillitoe, R.H., 2010. Porphyry copper systems. *Econ. Geol.* 105, 3–41.
- Sun, W.D., Xie, Z., Chen, J.F., Zhang, X., Chai, Z.F., Du, A.D., Zhao, J.S., Zhang, C.H., Zhou, T.F., 2003. Os–Os dating of copper and molybdenum deposits along the Middle and Lower Reaches of the Yangtze River, China. *Econ. Geol.* 98, 175–180.
- Sun, W.D., Arculus, R.J., Kamenetsky, V.S., Binns, R.A., 2004. Release of gold-bearing fluids in convergent margin magmas prompted by magnetite crystallization. *Nature* 431, 975–978.
- Wang, M.F., Gutzmer, J., Michalak, P.P., Guoa, X.N., Xiao, F., Wang, W., Liu, K., 2014. PGE geochemistry of the Fengshan porphyry-skarn Cu–Mo deposit, Hubei Province, Eastern China. *Ore Geol. Rev.* 56, 1–12.
- Wones, D.R., Eugster, H.P., 1965. Stability of biotite: experiment, theory and application. *Am. Mineral.* 50, 1228–1272.
- Xie, G.Q., Zhao, H.J., Zhao, C.S., Li, X.Q., Hou, K.J., Pan, H.J., 2009. Re–Os dating of molybdenite from Tonglushan ore district in southeastern Hubei Province, Middle–Lower Yangtze River belt and its geological significance. *Mineral Deposits* 28, 227–238 (In Chinese with English abstract).
- Xu, Y.M., Jiang, S.Y., Zhu, Z.Y., Zhou, W., Kong, F.B., Sun, M.Z., Xiong, Y.G., 2013. Geochronology, geochemistry and mineralogy of ore-bearing and ore-barren intermediate-acid intrusive rocks from the Jiuru ore district, Jiangxi Province and their geological implications. *Acta Petrol. Sin.* 29 (12), 4291–4310 (in Chinese with English abstract).
- Yang, S.Y., Jiang, S.Y., Li, L., Sun, Y., Sun, M.Z., Bian, L.Z., Xiong, Y.G., Cao, Z.Q., 2011. Late Mesozoic magmatism of the Jiuru mineralization district in the Middle-Lower Yangtze River Metallogenic Belt, Eastern China: precise U–Pb ages and geodynamic implications. *Gondwana Res.* 20, 831–843.
- Zhai, Y.S., Xiong, Y.L., Yao, S.Z., Lin, X.D., 1996. Metallogeny of copper and iron deposits in the Eastern Yangtze Craton, east-central China. *Ore Geol. Rev.* 11, 229–248.
- Zhao, K.D., Jiang, S.Y., Jiang, Y.H., Wang, R.C., 2005. Mineral chemistry of the Qitianling granitoid and the Furong tin ore deposit in Hunan Province, South China: implication for the genesis of granite and related tin mineralization. *Eur. J. Mineral.* 17, 635–648.
- Zhu, Z.Y., Jiang, S.Y., Jian, H., Gu, L.X., Li, J.W., 2014. Geochronology, geochemistry, and mineralization of the granodiorite porphyry hosting the Matou Cu–Mo (\pm W) deposit, Lower Yangtze River metallogenic belt, eastern China. *J. Asian Earth Sci.* 79, 623–640.